

The *Caenorhabditis elegans* ortholog of *C21orf80*, a potential new protein O-fucosyltransferase, is required for normal development

Olivier Menzel,^{a,1,2} Tibor Vellai,^{b,1} Krisztina Takacs-Vellai,^b Alexandre Reymond,^a Fritz Mueller,^b Stylianos E. Antonarakis,^a and Michel Guipponi^{a,*,3}

^aDivision of Medical Genetics, University of Geneva Medical School, 1 Rue Michel Servet, 1211 Geneva 4, Switzerland

^bInstitute of Zoology, University of Fribourg, Pérolles, CH-1700 Fribourg, Switzerland

Received 23 October 2003; accepted 5 April 2004

Available online 28 May 2004

Abstract

Down syndrome (DS), as a phenotypic result of trisomy 21, is the most frequent aneuploidy at birth and the most common known genetic cause of mental retardation. DS is also characterized by other phenotypes affecting many organs, including brain, muscle, heart, limbs, gastrointestinal tract, skeleton, and blood. Any of the human chromosome 21 (Hsa21) genes may contribute to some of the DS phenotypes. To determine which of the Hsa21 genes are involved in DS, the effects of disrupting and overexpressing individual human gene orthologs in model organisms, such as the nematode *Caenorhabditis elegans*, can be analyzed. Here, we isolated and characterized *C21orf80* (human chromosome 21 open reading frame 80), a potential novel protein O-fucosyltransferase gene that encodes three alternatively spliced transcripts. Transient expression of tagged *C21orf80* proteins suggests a primary intracellular localization in the Golgi apparatus. To gain insight into the biological role of *C21orf80* and its potential role in DS, we isolated its *C. elegans* ortholog, *pad-2*, and performed RNA interference (RNAi) and overexpression experiments. *pad-2(RNAi)* embryos showed failure to undergo normal morphogenesis. Transgenic worms with elevated dosage of *pad-2* displayed severe body malformations and abnormal neuronal development. These results show that *pad-2* is required for normal development and suggest potential roles for *C21orf80* in the pathogenesis of DS.

© 2004 Elsevier Inc. All rights reserved.

Down syndrome (DS), caused by trisomy 21, is the most common genetic cause of mental retardation, with an incidence of approximately 1 in 700 live births. DS patients show several clinical manifestations that affect multiple organs with variable penetrance. In addition to mental retardation and facial characteristics, there are numerous other phenotypes associated with DS, including heart disease and early onset Alzheimer disease [3]. The completion of the genomic sequence of human chromosome 21 (Hsa21) [12] and its mouse syntenic regions [23,31] is facilitating the discovery of the Hsa21 genes [2,7,26,27]. After the charac-

terization of the Hsa21 gene repertoire, the next issue is to uncover their functions and to determine which ones are involved in the phenotypes of DS [9,28]. Model organisms will be essential to determine the function of these genes by studying the functional/phenotypical effects of their inactivation and overexpression. The nematode *Caenorhabditis elegans* is an attractive experimental model organism to study gene function. Despite its apparent rudimentary organization, the main cell types affected in DS, including muscle cells and neurons, can be individually identified [1,30]. Importantly, approximately 25% of Hsa21 genes exhibit a high level of sequence homology to genes within the *C. elegans* genome [8].

Here, we report the isolation and initial characterization of *C21orf80*, a potential new protein O-fucosyltransferase that maps to Hsa21. Protein O-fucosyltransferase is an emerging class of enzymes that add O-fucose to conserved serine or threonine residues in the epidermal growth factor-like domains of a number of cell surface and secreted proteins. Recent studies have shown that signaling events

* Corresponding author

E-mail address: guipponi@wehi.edu.au (M. Guipponi).

¹ These two authors contributed equally to this work.

² Present address: Swiss Institute of Experimental Cancer Research, 155, Chemin des Boveresses, CH-1066 Epalinges sur Lausanne, Switzerland.

³ Present address: Genetics and Bioinformatics Division, The Walter and Eliza Hall Institute of Medical Research, Royal Parade, P.O. Royal Melbourne Hospital, Parkville, VIC 3050, Australia.

involved in development can be regulated by O-fucosylation [11]. To determine the biological role of *C21orf80* in development and its potential involvement in DS, its *C. elegans* ortholog *pad-2* was isolated and characterized. Both disruption and overexpression of *pad-2* revealed essential functions in normal development and suggested possible roles for *C21orf80* in the pathogenesis of DS.

Results

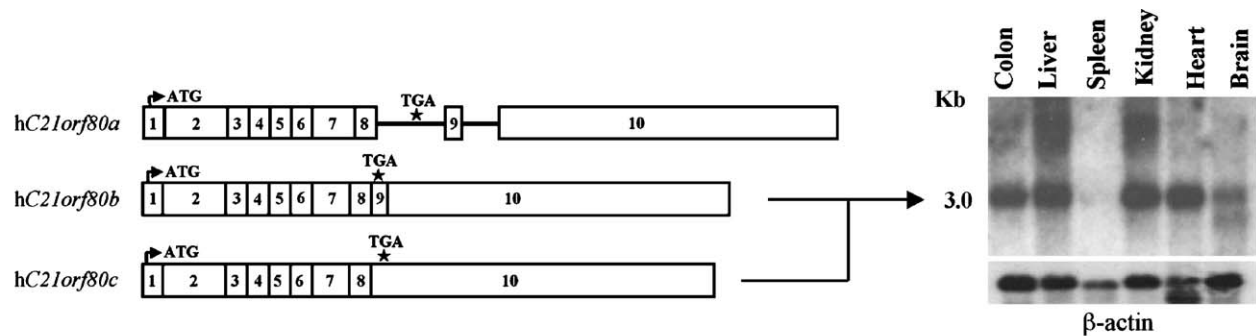
Isolation of the human C21orf80 gene and its C. elegans ortholog

In silico analysis of approximately 1 Mb of 21q22.3 genomic sequence revealed the existence of a new gene, subsequently named *C21orf80*. The *C21orf80* gene is composed of 10 exons and spans over 24 kb of genomic sequence between *ADARB1* and *COL18A1*. We identified three different alternatively spliced transcripts. *C21orf80a* (AJ302080) is a 424-amino-acid putative protein. This isoform results from introns 8 and 9 not being spliced. *C21orf80b* (AJ302079) contains all the exons, is 3055 bp in size, and

encodes a putative 380-amino-acid protein. *C21orf80c* (AY066015) results from the splicing out of exon 9, is 2849 bp in size, and encodes a putative 429-amino-acid protein (Fig. 1A). Homology searches against publicly available databases revealed that *C21orf80* is also known as *POFUT2* (FUT13; AJ575591), a member of a newly identified protein O-fucosyltransferase family, POFUT2 [20].

The human *C21orf80b* protein sequence was used to search the mouse, *Drosophila*, and *C. elegans* genome databases. A unique *C. elegans* ortholog of *C21orf80* (Z36282, ORF K10G9.3) was identified and confirmed by RT-PCR. It is composed of five exons, spans approximately 2 kb of genomic sequence, and encodes a putative protein of 426 amino acids that shows 45% identity to the human *C21orf80b* protein (Fig. 1B). No alternative transcripts were identified in *C. elegans*. The *C. elegans* ortholog of *C21orf80* was named *pad-2*, which stands for *C. elegans* patterning defective-2 (see later in the text [10]). The mouse *C21orf80* ortholog (AF455270) encodes a protein of 429 amino acids and shows 92% identity with the human *C21orf80b* protein. The *Drosophila* ortholog O-fucosyltransferase 2 (AAF45629) encodes a 490-amino-acid protein that shows 38% identity with the human *C21orf80b* protein.

A



B

```

HUMADS01 1 -----MATLSFVFLLLGAVSWPPASASG-----QEFWPGQSAADILSGAASRRRYLLYDVNPPPEGFNLRDRVYIRHA
MUMADS01 1 -----MAALSIVUCFLLAASRRPVSASG-----EFHWPGQSAADILSGAASRRRYLLYDVNPPPEGFNLRDRVYIRVA
C0MADS01 1 -----MFFPQLLLLPFAEKIAFEMS-----DQTVS-RVDSRRYS-VAAEKRLLYDVNPPPEGFNLRDRVYIRVA
CG14789-PA 1 MRGSHPRLGFPALLLLHLTGSDAVNRNGTAKREIGDSRGSSTGCVKGFLEPILPLPATCPEVLGMRGAVFLYDVNISEGFNLRDRVYIRMA

HUMADS01 68 SLKRLTLLKT--EEWVVLPPWGRLYHWQSPDIHQVRIIPWSEFFDLPPLSNKIPVIEYEQFHAES--GQP----FIDQVYVLC SYABGHWKEGT
MUMADS01 68 SLKRLTLLKT--EEWVVLPPWGRLEHWQSPDIHQVRIIPWSEFFDLPPLSNKIPVIEYEQFHAES--GQP----FIDQVYVLC SYABGHWKEGT
C0MADS01 66 NTVKSLRDSG--EHWLVLPPWGRLEHWKFR--NEUPLSGMLPFDLPSLRPLPVEEEDPDEET--EKR----FLDQVYVLC SYABGHWKEGT
CG14789-PA 96 VFVRRLLQRRRRFRHVRLVLLPPHRLYHWHSGQLQSGLPWSEHF DLA SLRR TAPVLDYE EFLAEQRLFGHGA PLVHVGHAFRLGHYEVML EQGI

HUMADS01 152 WEEKVDREPCIDQLL--YSQDKHEYRGWFWGYEETRGLNVSCLSVQGSASTVAPLLLRN-----TSARSVMLDRAENLLHDHYGGKREY
MUMADS01 152 WEEKVDREPCIDQLL--YSQDKHEYRGWFWGYEETRGLNVSCLSVQGSASTVADVLLRN-----TSARSVMLDRAENLLHDHYGGREY
C0MADS01 147 YVRKPERKSCLPFAESHKQVEEFKKKMTSELDVTSRNQCWSTQDSEGLTKDLKHSN-----FSESTSHVDRAETLLHSHYGVVDI
CG14789-PA 191 FRDKPERVTDKPCS-------GSLSGGPLLQQNELIVGGRFHCWRPQSSAGLLEKLLREAYDDEDTAGPEVDVDDNRYALLSAEYVLDHMGDEHF

HUMADS01 234 WDTRRSMVFAHRLRQVGFDFRSNHLNSTDAADRIFPQEDWTKMKV KLG SALGGPYLGVHLRKRDFIWHGRQDVPFSLGAVKIRSLMKTHTLQDKV
MUMADS01 234 WDTRRSMVFAHRLRAVGFDFRSQHLNSTDAADKNMAPPEDWTKMKV KLG SALGGPYLGVHLRKRDFIWHGRQEDVPFSLGAVKIRSLMKTHTLQDKV
C0MADS01 233 WKAARRSMYRNDLVQVADAFRKYLDSDDDRDNTKLVDDWENEPFR--TATGGPYLGHMRRNDPLTARAQQEPIPGTALNQLDQLCKLQLDQNE
CG14789-PA 279 HQARRSMFARALREQVADAFRRRQALDPTDASAGVQRPAMHLELRPKR--NARGGDYLCALRRQDQEVRSRPAATTEHKAQAQVQKQLLRGPHMTTY

HUMADS01 329 FVATDAVRKVEEELKLLF-EMVRFEPTEWEELEI--YKDGGAVIDQNICAHARFFIGTSVSTFSFRIHEEREILGLDPKITYNRFCGDQEKACE
MUMADS01 329 FVATDAVRKVEEELKLLF-EMVRFEPTEWEELEI--YKDGGAVIDQNICAHARFFIGTSVSTFSFRIHEEREILGLDPKITYNRFCGDQEKACE
C0MADS01 327 YLATDAPDQBEVDELRKALLNGBLEVYR--FDTQK--LNDGGAVIDQNICAHAAVFIGEYESTFTFRIQEDREILGFPISLTYNRFCGDPTEACE
CG14789-PA 373 FLATDAPDQBEVDELRKALLNGBLEVYR--FDTQK--LNDGGAVIDQNICAHARFVIGTVESTFTFRIRIHEEREILGFTQASGFNTPC KALGSGSG

HUMADS01 421 OPTHWKLIAY-----
MUMADS01 421 OPTHWKLIAY-----
C0MADS01 418 OPAKWKIVY-----
CG14789-PA 468 RNAVWPIVWADGDSSEEDSDPY
    
```

Fig. 1. (A) Schematic representation of the three *C21orf80* mRNA isoforms identified. Exons are represented as numbered boxes, introns are shown as thin lines, start and stop codons are indicated. Two different mRNA species of 3.0 and 2.3 kb were detected. Northern blot analysis was performed using a probe designed to detect all three *C21orf80* mRNA isoforms. (B) Multiple sequence alignment of the deduced amino acid sequence of the human *C21orf80b* (AJ302079), the mouse *C21orf80* ortholog (AF455270), the *C. elegans C21orf80* ortholog (AF455271), and the *Drosophila* ortholog O-fucosyltransferase 2 CG14789-PA (AAF45629). The mouse *C21orf80* cDNA was isolated by assembling ESTs (BG915839, B1646651, A1550762). Identical amino acids are shaded in black. Conserved amino acids are shaded in gray.

Expression pattern and intracellular localization of *C21orf80*

Northern blot analysis revealed a ubiquitous band of approximately 3 kb that could correspond to *C21orf80b* and/or *c*. A faint 2.5-kb band was also observed in brain (Fig. 1A). RT-PCR was performed on a panel consisting of 24 human cDNA samples [28] to determine the expression profile of each of the three *C21orf80* transcripts. *C21orf80a* was found to be expressed in fetal liver and peripheral blood lymphocytes. *C21orf80b* was detected in spleen, lung, testis, bone marrow, fetal brain, fetal liver, fetal kidney, thymus, pancreas, and prostate. *C21orf80c* was detected in brain, heart, spleen, liver, lung, stomach, testis, placenta, skin, fetal brain, fetal liver, fetal heart, thymus, pancreas, mammary gland, and prostate (data not shown).

To determine where *C21orf80* might exert its cellular function, EGFP–*C21orf80* or HA–*C21orf80* proteins were expressed in COS-7 and U2OS cells. In both cell types, *C21orf80* proteins were found in the cytoplasm chiefly in one or more perinuclear spots (Fig. 2). To define better the compartments identified by *C21orf80* proteins, colocalization experiments were performed in COS-7 cells using markers specific for the Golgi apparatus, the endoplasmic reticulum, and the microtubule network. The results showed that *C21orf80* proteins colocalize to some extent with Giantin, a Golgi apparatus-specific protein (Fig. 2, data not shown for *C21orf80a* and *c*).

pad-2(RNAi) embryos show patterning defects

We used RNA-mediated interference (RNAi) to investigate the role of *pad-2*, the *C. elegans* ortholog of *C21orf80*, in development. *pad-2*, previously described as a predicted gene (K10G9.3), had not been considered a genuine ORF and thereby avoided large-scale RNAi screening. Feeding worms with bacteria expressing *pad-2* double-stranded RNA (dsRNA) caused embryonic lethality at an average penetrance of 17% (Table 1). The affected *pad-2(RNAi)* embryos arrested growth and development at various stages, beginning at the onset of morphogenesis, when terminal differentiation occurs [15,30]. They also displayed obvious body malformations owing to the failure in embryonic patterning and elongation (Figs. 3B, 3D, 3G, and 3K). The presence of autofluorescent gut granules (Fig. 3B) as well as the expression of the epidermal marker *jam-1::gfp* (Fig. 3H), the neuron-specific *unc119::gfp* (Fig. 3L), and the body wall muscle reporter *myo-3::gfp* (data not shown) suggested that at least some cell types were properly differentiated in *pad-2(RNAi)* embryos [6,18,22]. However, the gut granules were mislocalized at the periphery of the arrested embryos (Figs. 3A and 3B), the epidermal cells were tightly clustered and displayed abnormal size and shape (Figs. 3F and 3H), and the prospective ventral nerve cord was either absent or mislocalized in 10% of the *pad-2(RNAi)* embryos (Figs. 3J and 3L). The body wall muscle marker *myo-3::gfp* also indicated,

although with a moderate penetrance, cell patterning defects. These data demonstrate that *pad-2* is required for embryonic morphogenesis by controlling body elongation and positioning of several cell types, including intestinal, hypodermal, body wall muscle, and neuronal cells.

Inactivation of *pad-2* by RNAi disrupts cellular integrity and decreases fertility

pad-2 dsRNA treatment caused a highly variable and incomplete penetrant phenotype during postembryonic development. Approximately ~2% of *pad-2(RNAi)* animals arrested development at different larval stages or at young adulthood, exhibiting severe body malformations (data not shown). The viable *pad-2(RNAi)* larvae and adults were characterized by loss or significant reduction of UNC-119::GFP staining in the ventral nerve cord neurons (Fig. 4B) and in other neuronal cells (not shown). Upon differential interference contrast microscopy, the majority of these neurons did not show signs of degeneration during development but rather an irregular size and position. The integrity of the axonal bundles also appeared to be disrupted. Furthermore, using the *myo-3::gfp* marker highlighting myosin heavy chain A, structural changes in the body wall muscle cells of *pad-2(RNAi)* worms were observed. In wild-type animals, the muscle cell sarcomeres were organized in tight parallel symmetric rows (Fig. 4C). In *pad-2(RNAi)* worms the sarcomeres became disorganized with marked signs of irregular orientation (Fig. 4D). Changes in neuronal or muscle cell structure, or both, can explain the egg-laying-defective (Egl) phenotype (<5%) observed in *pad-2(RNAi)* hermaphrodites (not shown). Occasionally, *pad-2(RNAi)* hermaphrodites displayed obvious defects in vulval development owing to abnormal orientation of vulval cell division (data not shown), which might have contributed to the observed Egl and/or everted vulva phenotypes.

The fertility of *pad-2(RNAi)* hermaphrodites was highly reduced. We found a mean “brood size” (all laid eggs) of 96 ± 16.5 in *pad-2(RNAi)* adults versus 191 ± 14.5 in wild-type animals. A portion of the oocytes produced by the RNAi-treated animals remained unfertilized after passing through the spermatheca (Fig. 4F). Although the spermatozooids looked normal, their number was significantly lower in 7 of 10 *pad-2(RNAi)* hermaphrodites (85–135 spermatozooids/spermatheca in *pad-2(RNAi)* hermaphrodites in contrast to 170–195 in wild-type animals, $n = 10$). A similar phenomenon was observed in *pad-2(RNAi)* males (data not shown), indicating that *pad-2* affects spermatozoid differentiation in both sexes.

Overexpression of *pad-2* affects morphogenesis

In an effort to dissect the potential implication of three copies of *C21orf80* in DS, we have evaluated the effect of an increased dose of *pad-2* on *C. elegans* development.

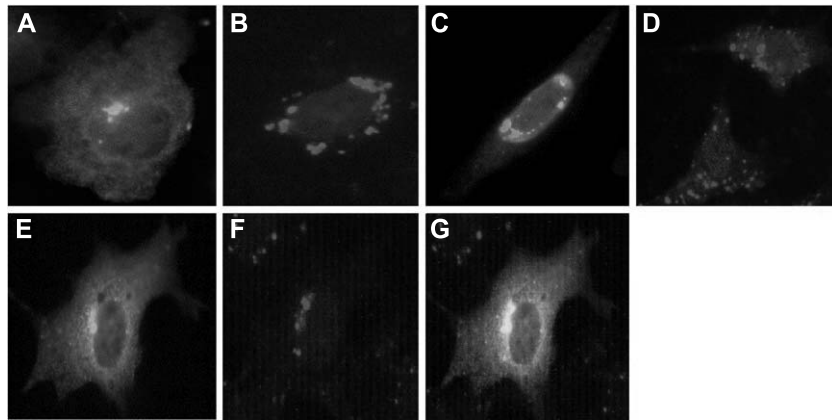


Fig. 2. Intracellular localization of the C21orf80 protein. Fluorescence microscopic analysis of fixed COS-7 or U2OS cells transiently transfected with (A) EGFP-C21orf80 (COS-7 cells, green signal), (B) HA-TMPRSS3 (COS-7 cells, red signal), (C) EGFP-C21orf80 (U2OS cells, green signal), and (D) HA-C21orf80 (U2OS cells, red signal) and counterstained with 4',6-diamidine-2'-phenylindole dihydrochloride (A, B, C, and D, blue signal). Fixed COS-7 cells transiently transfected with (E) EGFP-C21orf80 (green signal) and (F) counterstained with Golgi apparatus marker (anti-Giantin antibody, red signal). (G) Colocalization of EGFP-C21orf80 with Golgi marker.

Overexpression of *pad-2* from a heat-inducible promoter that is active in almost all somatic cells [5] caused a highly penetrant embryonic lethality (83%, Table 2) accompanied by severe body malformations, indicating that embryonic

cells are sensitive to excessive and/or ectopic *pad-2* dosage. The developmental stage at which the affected embryos arrested growth varied highly among individuals. To restrict the overexpression of *pad-2* to the appropriate tissues and to

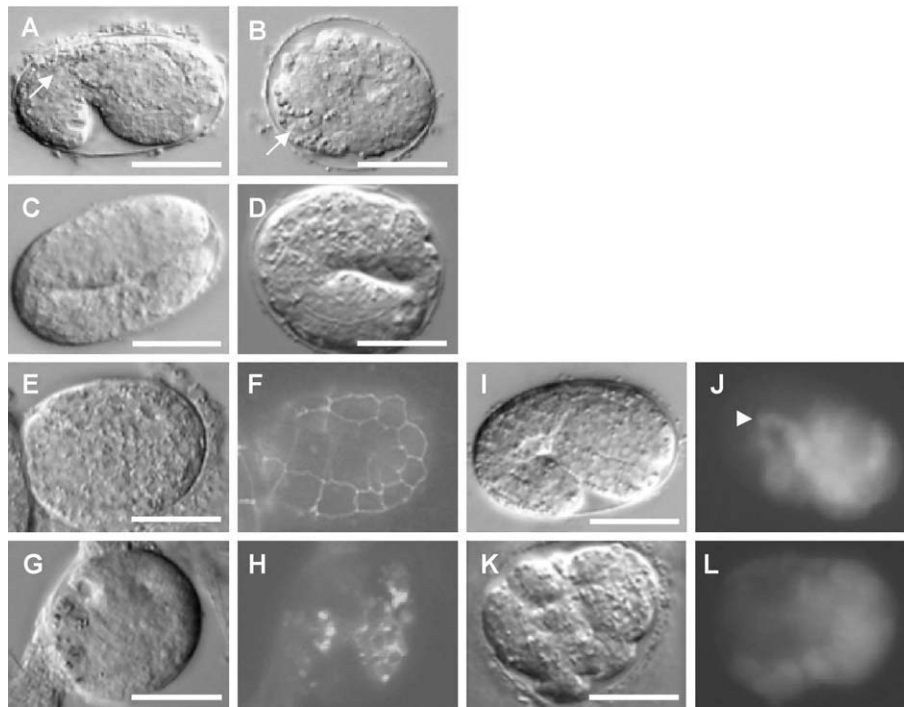


Fig. 3. Depletion of *pad-2* by RNAi causes defects in embryonic patterning. (A) Differential interference contrast (DIC) image of a comma stage (390 min) wild-type embryo and (B) a 390-min *pad-2(RNAi)* embryo that failed to undergo elongation. Arrows point to the autofluorescent gut granules that are located abnormally to the periphery in the *pad-2(RNAi)* embryo. (C) DIC image of a wild-type and (D) a *pad-2(RNAi)* 2-fold-stage embryo. (E) DIC image and (F) corresponding fluorescence micrograph of a 350-min wild-type embryo transgenic for the epidermal adherent junction marker *jam-1::gfp*. (G) DIC and (H) fluorescence images of a 380-min *pad-2(RNAi)* embryo. The hypodermal (green) and intestinal (yellowish) cells are tightly clustered. (I) DIC image and (J) corresponding fluorescence micrograph of a 1.5-fold-stage (400-min) wild-type embryo bearing the neuronal marker *unc-119::gfp*. (K) DIC and (L) fluorescence images of a 400-min *pad-2(RNAi)* embryo transgenic for *unc-119::gfp*. Mislocalization of the prospective ventral nerve cord (indicated by an arrowhead in J in the wild type) is evident. The RNAi-treated embryos shown in B, D, G/H, and K/L arrested growth and development at different stages. Bars represent 20 μ m.

Table 1
Lethality of *pad-2(RNAi)* embryos

Bacterial strain used for feeding	No. of embryos examined	% of dead embryos	% of viable embryos
HT115(DH3) (control)	1410	6.6	93.4
HT115(DH3) <i>pad-2</i> dsRNA	2119	23.9	76.1

levels observed in trisomy 21, we injected the cosmid K10G9, which contains the *pad-2* coding region and 3 kb of upstream regulatory sequences, into wild-type animals. Consistent with the heat-shock data, animals transgenic for K10G9 showed a moderate percentage of embryonic lethality (5.1%, Table 2) and early larval arrest characterized by mild to severe morphogenetic abnormalities (Figs. 5A, 5B, 5D, and 5E). Although the K10G9-transgenic arrested animals exhibited almost normal body elongation and tissue differentiation, they showed obvious patterning defects that were manifested in severe body malformations mainly in the head and tail as well as in protrusions along the entire anteroposterior body axis.

Levels of transgene expression were estimated by semiquantitative PCR that showed increased dose of *pad-2* mRNA in both transgenic strains (*hs::pad-2* and cosmid K10G9) compared to wild-type animals (Fig. 5F). It must be noted that we could not formally exclude the possible effect of K10G9.2, the only other full-length gene present in cosmid K10G9, on the observed phenotype. However, overexpressing *pad-2* under a heat shock promoter or its own promoter resulted in the same phenotype characterized by embryonic lethality associated with various morphological defects. Furthermore, consistent with the level of *pad-2* overexpression, the penetrance of this phenotype was much higher when *pad-2* was overexpressed under a heat shock promoter. Taken together, our experimental results indicate that embryonic lethality in animals trans-

genic for cosmid K10G9 was caused by extra copies of *pad-2*.

To evaluate the effects of elevated *pad-2* dose on cell fate determination, we examined the expression of the neuronal marker *unc-119::gfp* in animals transgenic for K10G9. Interestingly, we detected a more intense and ectopic UNC-119::GFP accumulation in the K10G9 transgenic embryos compared with the wild-type expression pattern (Figs. 5G–5N). For example, the border of the UNC-119::GFP-positive area in the head was slightly shifted toward the posterior pole. Furthermore, certain neurons, for example those that belong to the ventral nerve cord, expressed UNC-119::GFP at abnormally high levels. This observation is consistent with the characterization of the *pad-2* RNAi phenotype, which revealed a faint and reduced UNC-119::GFP expression relative to that found in the wild type. These data suggest that *pad-2* influences cell identity at least in neurons in a dosage dependent manner.

pad-2 is expressed in different cell types from morphogenetic embryonic stages throughout development

The expression pattern of *pad-2* was analyzed by using animals carrying a *pad-2::gfp* reporter, *swEx571*, tagged with a nuclear localization signal. Consistent with the observed *pad-2* RNAi phenotypes, *pad-2* expression starts during the morphogenetic period of embryonic development. At this stage it was detectable in the anterior part of the embryos, in the hypodermal and neuronal cells of the head (Fig. 6A). After the animal hatched, *pad-2* was expressed at different levels in a variety of cell types, including neuronal, hypodermal, muscle, intestinal, and somatic gonadal cells (Fig. 6C and data not shown). PAD-2::GFP accumulation was most intense in the nerve ring around the pharynx (Fig. 7A), in the dorsal and ventral nerve cords (Fig. 7B), in the intestine, and in a variety of hypodermal cells (Fig. 7C) of the L1–L3-stage larvae. In

Fig. 4. *pad-2* RNAi affects the integrity of neuronal and body wall muscle cells and reduces fertility. (A) Ventral nerve cord (arrow) in a wild-type L4-stage larva expressing the neuronal marker UNC-119::GFP. (B) Many of the ventral cord neurons failed to express UNC-119::GFP in a *pad-2(RNAi)* L4 larva. The integrity of the axonal bundles is also disrupted (arrow). (C and D) Fluorescence micrographs showing a body wall muscle cell from a wild-type and a *pad-2(RNAi)* L4 larva, respectively. Both animals are transgenic for the body wall muscle marker *myo-3::gfp*. Sarcomeres are organized in tight symmetric parallel rows in the wild-type animal, whereas they reflect irregular orientation in the *pad-2* RNAi-treated animal. (E and F) DIC images of wild-type and *pad-2(RNAi)* hermaphrodites, respectively. The white-filled arrow shows the vulva, the black arrow points to the spermatheca. As the oocytes pass through the spermatheca, they start to divide in the wild-type animals but remain unfertilized in the *pad-2(RNAi)* animals. Bars represent 20 μ m in A, B, E, and F and 10 μ m in C and D.

Fig. 5. Elevated dosage of *pad-2* causes defects in morphogenesis and influences the expression of the neuronal marker UNC-119::GFP. (A) Wild-type 420-min-stage embryo. (B) Arrested 420-min-stage embryo transgenic for the cosmid K10G9 shows severe morphogenetic defects. (C) Wild-type L1 larva. (D, E) L1 larvae transgenic for K10G9 display mild or severe body malformations. (F) Semiquantitative RT-PCRs were performed to determine the levels of *pad-2* mRNA in (lane 1) wild-type animals and (lane 2) *hs::pad-2* and (lane 3) K10G9 transgenic animals. The ubiquitously expressed *ama-1* mRNA (426 bp) was used as an internal control. Strains transgenic for *hs::pad-2* and K10G9 show an elevated level of *pad-2* mRNA relative to wild-type animals (lane 1). (G, H) DIC and fluorescence images of a gastrula transgenic for *unc-119::gfp*. (I, J) Embryo at the same stage as in G and H is transgenic for both K10G9 and *unc-119::gfp*. (K, L) Comma-stage embryo transgenic for *unc-119::gfp*. (M, N) Comma-stage embryo transgenic for both K10G9 and *unc-119::gfp*. The presence of K10G9 causes ectopic and more intense UNC-119::GFP expression relative to that found in the wild type. (G, I, K, M) DIC images and (H, J, L, N) corresponding fluorescence images. The epifluorescence images were captured with the same exposure time. Anterior is left, dorsal up. Bars represent 20 μ m.

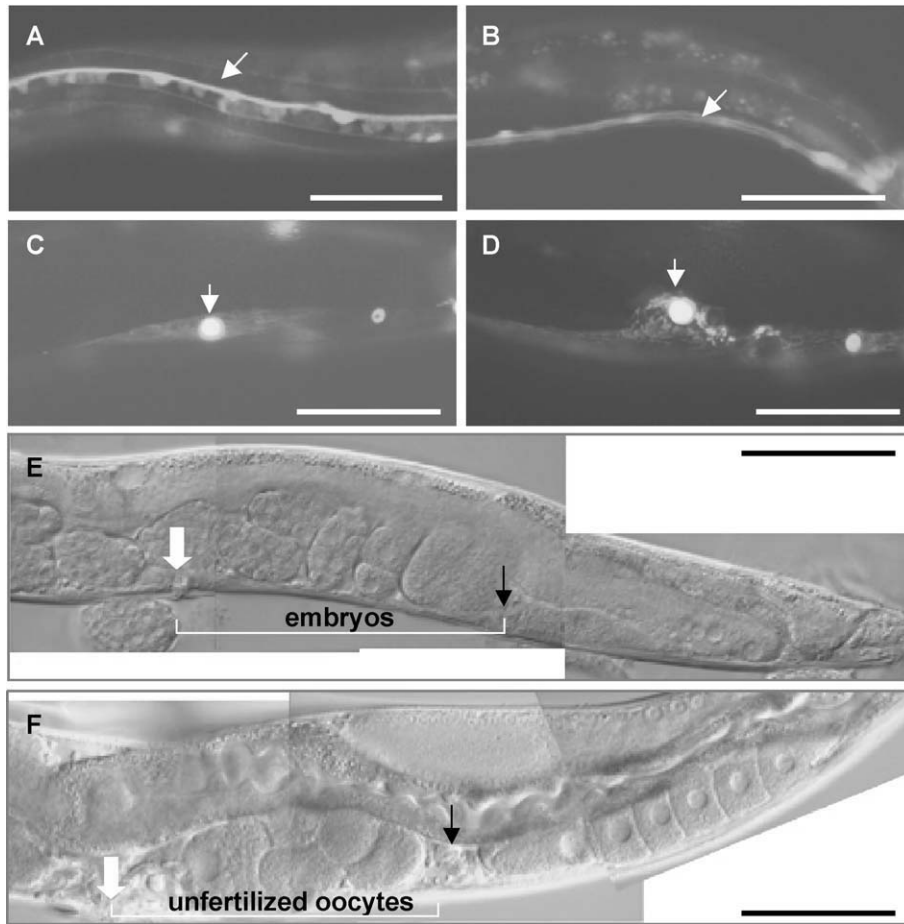


Fig. 4.

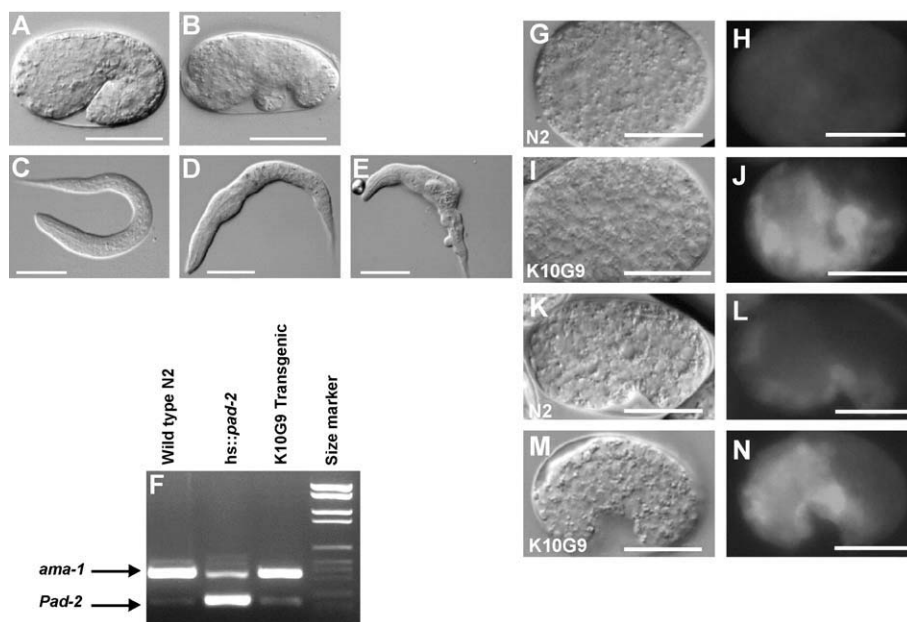


Fig. 5.

Table 2
Overexpression of *pad-2* results in embryonic arrest

Strains	No. of eggs examined	% of embryonic lethality
N2 ^a without heat shock	Many	0.5
N2 with heat shock	713	10.1
FR710 ^b without heat shock	956	3.2
FR710 with heat shock	1228	86
FR711 ^c	742	5.1

^a Wild-type strain.

^b Strain transgenic for the *hs::pad-2/rol-6* array.
Strain transgenic for the cosmid K10G9.

adult hermaphrodites, gonadal sheath cells, spermatheca, and tissues surrounding the vulva showed intense *pad-2* expression (Fig. 7D). These observations are consistent with sterility and vulva-specific phenotypes found in *pad-2(RNAi)* hermaphrodites. PAD-2::GFP was also expressed in the body wall muscle and hypodermal cells in both sexes (Figs. 7F and 7G).

Discussion

Down syndrome is a complex disorder caused by trisomy of Hsa21. The current hypothesis for how trisomy 21 leads to DS is that some genes, but not all, contribute to aspects of the DS phenotype. Clarifying the roles of individual Hsa21 genes in DS requires both overexpression and knockout approaches in model organisms. Here, we describe the isolation and initial characterization of *C21orf80*, a potential new protein O-fucosyltransferase. *C21orf80* is ubiquitously expressed in human tissues and may primarily localize in the Golgi apparatus, two characteristics of many other glycosyltransferases [14]. High level of homology among human, mouse, *Drosophila*, and *C. elegans* *C21orf80* proteins indicates an evolutionarily conserved biological role. Recent studies have provided evidence of a role for O-fucosylation in signal pathways involved in development [11]. The most remarkable example is the demonstration that O-fucose modification by protein O-fucosyltransferase (OFUT1) is essential for most, and possibly all, aspects of Notch signaling [24,25]. Based on these results, we hypothesize that overexpression of *C21orf80* in DS could lead to variation in the profile of O-fucosylation on target proteins, influencing their function by eliciting a new conformational change or masking or creating new recognition sites between proteins.

To investigate the biological role of *C21orf80* and its potential involvement in DS, we isolated its *C. elegans* ortholog, *pad-2*. Downregulation of *pad-2* resulted in a pleiotropic phenotype observed at different stages of development. Consistent with the onset of *pad-2* expression during the morphogenetic period of embryonic development, affected *pad-2(RNAi)* embryos failed to

undergo normal morphogenesis and showed arrested development. A more detailed analysis of the embryonic phenotype revealed abnormal positioning of several cell types without apparently affecting tissue differentiation. For example, the prospective ventral nerve cord, the intestine, the hypodermis, and the body wall muscle cells were mislocalized or partially formed in a fraction of *pad-2(RNAi)* embryos.

Most of the tissues expressing *pad-2* at the larval and adult stages were affected upon RNAi, although the penetrance of postembryonic phenotypes was highly incomplete. *pad-2(RNAi)* adult hermaphrodites displayed abnormal vulval development and reduced fertility, consistent with strong *pad-2* expression in developing vulval tissue of L3 and L4 stage larvae and in the gonadal sheath cells and spermatheca of adult hermaphrodites. These observations suggest that *pad-2* is involved in vulval cell fate specification as well as germ cell generation. *pad-2(RNAi)* larvae also showed obvious cell fate specification defects in certain neurons, especially in the ventral nerve cord, consistent with strong expression of *pad-2* in these cells. This suggests a role for *pad-2* in neuronal development and survival. *pad-2* is also required for the integrity of body wall muscle cells by controlling the orientation of sarcomeres. Even observed at incomplete penetrance, these phenotypes were considered significant as they were reproducible and never observed in wild-type animals.

Overexpression of *pad-2* under the control of a heat shock promoter that is active in most somatic cells resulted in highly penetrant embryonic lethality, indicating that the correct dose of *pad-2* is critical for normal development. However, strong overexpression of many genes in a nonphysiological manner will almost certainly result in an apparent phenotype [19,32]. Therefore, transgenic worms were generated with the cosmid K10G9, which contains *pad-2* and its endogenous regulatory sequences. K10G9 transgenic animals also showed embryonic lethality and morphogenetic defects. Our findings suggest that a correct dosage of *pad-2* is necessary for normal development.

C. elegans neuronal development was affected in both *pad-2(RNAi)* and K10G9 transgenic embryos. Notably, *pad-2* downregulation or overexpression caused disorganization of the developing neuronal network in the opposite manner. Absence of *pad-2* resulted mostly in the loss or reduced expression of a neuronal marker, whereas *pad-2* overexpression seemed to activate neuronal proliferation and/or specification. This implies that *pad-2* may act as a coordinator of cell fate specification and tissue patterning during embryonic neural development.

Interestingly, the gene defective in leukocyte adhesion deficiency II (LADII) encodes a putative GDP-fucose transporter [16,17]. The fucosylation of glycoproteins was found to be defective in individuals with LADII who suffer from severe infections, persistent leukocytosis, short stature, unusual facial and skeletal abnormalities,

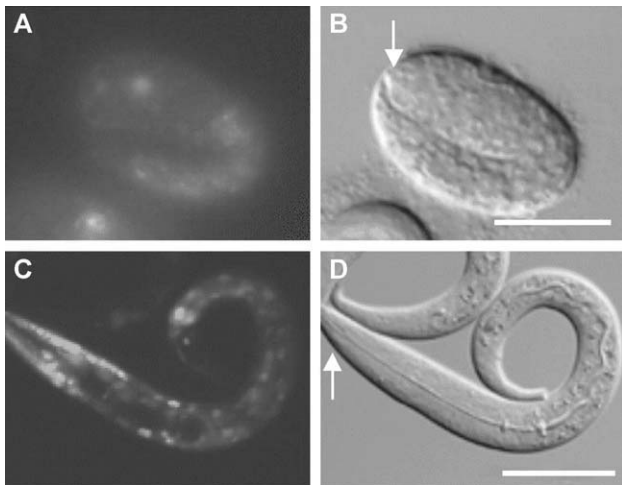


Fig. 6. Early expression of *pad-2* during *C. elegans* development. *pad-2* is expressed ubiquitously from the onset of embryonic morphogenesis throughout development. (A) Fluorescence micrograph of a 2-fold-stage embryo expressing PAD-2::GFP. PAD-2::GFP fluorescence is detectable in the anterior part of the body. (C) L1 larva showing PAD-2::GFP accumulation in different cell types, including hypodermal, intestinal, neuronal, and muscle cells. (B, D) Corresponding DIC images of the same animals. The yellowish color in A indicates gut autofluorescence. White arrows in B and D point to the head. Bars represent 20 μm .

and severe mental retardation pointing to the importance of fucosylation for the development of the neuronal system.

Taken together, these results suggest a potential role for *C21orf80* in DS phenotypes.

Materials and methods

Isolation of the human *C21orf80* cDNA and gene

Detailed analysis of 21q22.3 genomic DNA (GenBank Nos. AL163300, AL163301, and AL163302) was performed using numerous computer programs, interfaced by NIX (<http://www.hgmp.mrc.ac.uk/NIX/>), a program that integrates most of the gene identification programs. Subsequently, 5'- and 3'-RACE and RT-PCR reactions were performed on human brain, placenta, and liver cDNAs using primers designed within predicted exons of a novel gene named *C21orf80*. The sequence of the primers used is available at <http://www.medgen.unige.ch>. The genomic structure and intron–exon junctions of *C21orf80* were determined by comparison of the genomic sequence with the cDNA sequences by using *est_genome* software (<http://www.hgmp.mrc.ac.uk>). *C21orf80* protein sequences were analyzed using the Tools and software packages at the Expaty Molecular Biology Server (<http://au.expaty.org/>).

Expression pattern of *C21orf80*

Northern blot analysis was performed on a commercially available blot (Origene Technologies, Rockville, MD, USA) containing 2 μg of poly(A)⁺ RNA from six adult tissues according to the manufacturer's recommendations. A partial cDNA clone spanning exons 4 to 9 of the *C21orf80b* transcript was used as a probe. The absence of *C21orf80* transcript in spleen is likely to be due to the very low quantity of spleen mRNA blotted on the membrane as

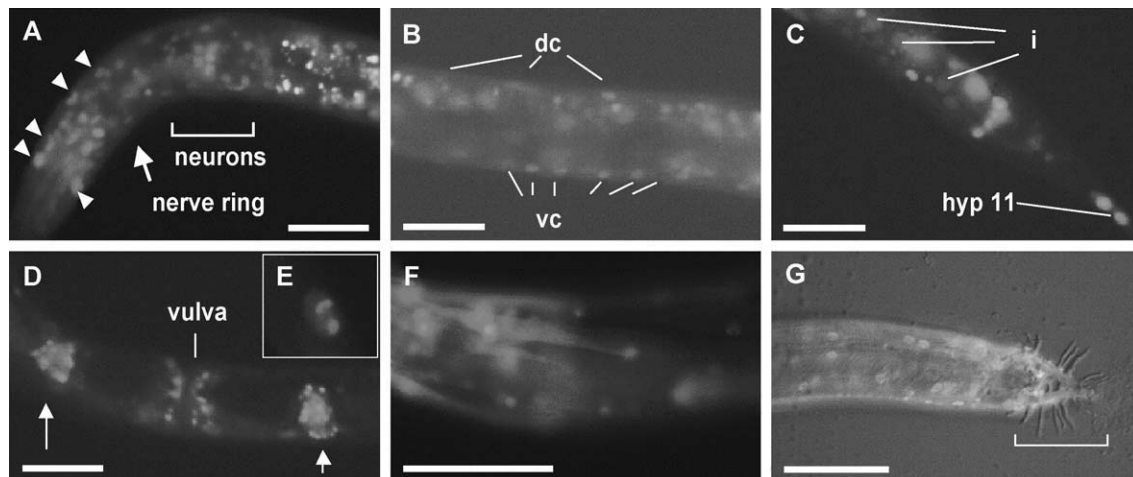


Fig. 7. Expression of *pad-2* in larval and adult stages. (A, B, C) Fluorescence micrographs showing PAD-2::GFP accumulation in the anterior, middle, and posterior body part of L2 larvae, respectively. (A) In the head, PAD-2::GFP is detectable in the nerve ring (arrow) and in the anterior hypodermal cells, hyp 3–6 (arrowheads). (B) In the midbody region, neurons that belong to the dorsal and ventral nerve cords indicated as dc and vc express *pad-2*. (C) PAD-2::GFP also accumulates in all intestinal (i) and many hypodermal cells (hyp 11). (D) Expression of *pad-2* in a young adult hermaphrodite. Vulval cells show intense PAD-2::GFP accumulation. Arrows point to the spermatheca where *pad-2* is also active. (E) Enlarged nucleus of a *pad-2::gfp*-expressing cell showing the presence of discrete foci of fluorescence that appear over the more diffuse background fluorescence. (F) *pad-2* is intensely expressed in the body wall muscle sarcomeres. (G) PAD-2::GFP accumulation in the posterior body part of an adult male shows *pad-2* expression in hypodermal, muscle, and neuronal cells. The bracket indicates the tail (rays). Bars represent 40 μm .

shown by the weak signal obtained with the β -actin control probe. RT-PCR was performed on a panel consisting of 24 human cDNA samples prepared as described [28]. The sequences of the primers used in this analysis are available on our Web page: <http://www.medgen.unige.ch/>.

Intracellular localization of *C21orf80* proteins

To visualize the intracellular localization of the *C21orf80* proteins, COS-7 and U2OS cells were transiently transfected with vectors expressing either 5'EGFP- or 5'HA-tagged *C21orf80* proteins as previously described [29]. To perform colocalization with known subcellular compartments, transfected COS-7 and U2OS cells were incubated with antibodies recognizing specific cellular structures: Golgi by a mouse anti-Giantin antibody (Calbiochem, San Diego, CA, USA); anti- α , - β , and - δ tubulin antibodies (Sigma–Aldrich, Munich, Germany), and the dye Endoplasmic Reticulum-Tracker Blue-White DPX (Molecular Probes, Eugene, OR, USA).

Isolation of *pad-2* cDNA, the *C. elegans* ortholog of *C21orf80*

The *C. elegans* ortholog of the human *C21orf80* gene was identified by tBLASTn using the human protein sequence against the *C. elegans* genomic DNA sequence. The full-length coding sequence of *pad-2* was isolated by RT-PCR using *C. elegans* poly(A)⁺ RNA. The genomic structure and intron–exon junctions of *pad-2* were determined by comparison of the genomic sequence with the cDNA sequence by using *est_genome* software (<http://www.hgmp.mrc.ac.uk>). The sequence of the primers used is available at <http://www.medgen.unige.ch>.

C. elegans strains, alleles, and general methods

C. elegans strains were maintained using standard methods [1]. Wild-type worms correspond to *C. elegans* var. Bristol, strain N2. Other strains were FR709 *swEx573[hs::pad-2 + rol-6(su1006)]*; FR710 *swEx574[hs::pad-2 + rol-6(su1006)]*; DP132 *edIs[unc-119::gfp + rol-6(su1006)]IV*; FR711 *swEx575[K10G9 + rol-6(su1006)]*; FR706 *swEx571[pad-2::gfp + ro-6(su1006)]*; FR707 *swEx572[pad-2::gfp + ro-6(su1006)]*; FR775 *Ccls4251[myo-3::gfp + dpy-20(+)]V*, *dpy-20(e1362)IV*; su93 *jcIsI[jam-1::gfp + rol-6(su1006) + unc-29(+)]IV* [22]; and DP132 *edIs[unc-119::gfp + rol-6(su1006)]IV* [18]. The *unc-119::gfp*, *myo-3::gfp* and *jam-1::gfp* reporters were used as neuronal, muscle, and epidermal markers, respectively. The strain expressing the *hs::pad-2/rol-6* array was maintained at 15°C, other strains were analyzed at 22°C.

RNAi assay

A 951-bp fragment of the *pad-2* cDNA was amplified by RT-PCR using primers 5'-CCGCTCGAGCG-

GACCGTGTCTCGGGTGGACTCGAAC-3' and 5'-[GGACTAGTCCAACAGAGCTTTGAGCTCATCGAC-3' and subcloned into pPD129.36 [6]. This construct, called pGEN1, was transformed into HT115(DE3) *Escherichia coli* strain. Bacteria containing pGEN1 were grown and induced as described [13], then seeded directly onto nematode growing medium (NGM) plates with 1 mM IPTG and 50 μ g/ml ampicillin. To examine the effects of *pad-2* RNAi, wild-type L4-stage larvae were transferred onto NGM plates seeded with bacteria that were expressing *pad-2* dsRNA, and the F1 siblings were analyzed.

Overexpression of *pad-2*

The *pad-2* cDNA was digested with restriction enzymes *NheI/KpnI* and cloned into pPD49.83, which contains the *C. elegans hsp16-41* heat-inducible promoter [4]. This construct, called pGEN2 (*hs::pad-2*), was co-injected with pRF4 carrying the dominant transformation marker gene *rol-6(su600)* at 50 ng/ μ l concentration into young adult hermaphrodites as previously described [21]. Worm lines transgenic for the *hs::pad-2/rol-6* array were established (strains FR709 and FR710) and heat shocked three or four times, each round being 33°C for 30 min followed by 20°C for 3 h and 30 min. The cosmid K10G9, which contains *pad-2(K10G9.3)* and its upstream regulatory sequences (<http://www.wormbase.org>), was also injected into young hermaphrodites, and a transgenic line (strain FR711) was established. To examine neuronal development in K10G9 transgenic animals, the strains FR711 and DP132 (*unc-119::gfp*) were crossed.

Analysis of *pad-2* overexpression was performed by RT-PCR. Total RNA was isolated from 30 wild-type, *hs::pad-2* transgenic, or K10G9 transgenic L4-stage larvae. *pad-2* and *ama-1* mRNAs were amplified by the Qiagen one-step RT-PCR system using primers 5'-AAATTTCGAGAAACG-GAGCTG-3' and 5'-TACTCCTTCTCGCCTTCCAG-3' for *pad-2*, 5'-CAGTGGCTCATGTTTCGAGT-3' and 5'-CGACCTTCTTCCATCAT-3' for *ama-1*. PCR products were separated on agarose gel and transgene expression levels were estimated using the respective intensity of the ethidium bromide bands using the Multi-Analyst software (Bio-Rad).

Expression analysis of *pad-2*

A 5-kb genomic fragment containing the first three exons of *pad-2* and 3 kb of upstream sequence (the closest upstream gene, *R01H10.8*, is located 2 kb from *pad-2*) was cloned into pPD95.69 (provided by A. Fire). This construct, called pGEN3, expresses the PAD-2::GFP fusion protein tagged with a nuclear localization signal under the control of the *pad-2* endogenous promoter. pGEN3 was co-injected with pRF4 into wild-type hermaphrodites. Two transgenic lines (FR706 and FR707) were established and examined using a Leica DM RXA epifluorescence micro-

scope equipped with DIC optics. Images were taken with a Hamamatsu chilled CCD camera (C5985) and processed with the Argus-20 Image Processor (Hamamatsu) using Adobe PhotoShop (4.0).

Acknowledgments

This project was supported by grants from the Jérôme Lejeune Foundation to A.R. and M.G.; the Swiss National Science Foundation, the National Center for Competence in Research “Frontiers in Genetics,” and the Child Care Foundation to S.E.A.; and Grant SNF 31-56953.99 to F.M. We are grateful to Andy Fire (Carnegie Institute of Washington) for the vectors pPD129.36 and pPD95.69, to Alain Coulson (Sanger Centre, Cambridge) for the cosmid K10G9, and Alessandro Puoti (University of Fribourg) for *C. elegans* poly(A)⁺ RNA.

References

- [1] S. Brenner, The genetics of *Caenorhabditis elegans*, *Genetics* 77 (1974) 71–94.
- [2] M.T. Davison, L.J. Bechtel, E.C. Akesson, A. Fortna, D. Slavov, K. Gardiner, Evolutionary breakpoints on human chromosome 21, *Genomics* 78 (2001) 99–106.
- [3] C.J. Epstein, Down syndrome (trisomy 21), in: C.R. Scriver, A.L. Beaudet, W.S. Sly, D. Valle (Eds.), *The Metabolic and Molecular Bases of Inherited Disease*, McGraw–Hill, New York, 1995, pp. 749–794.
- [4] A. Fire, D. Albertson, S.W. Harrison, D.G. Moerman, Production of antisense RNA leads to effective and specific inhibition of gene expression in *C. elegans* muscle, *Development* 113 (1991) 503–514.
- [5] A. Fire, S.W. Harrison, D. Dixon, A modular set of lacZ fusion vectors for studying gene expression in *Caenorhabditis elegans*, *Gene* 93 (1990) 189–198.
- [6] A. Fire, S. Xu, M.K. Montgomery, S.A. Kostas, S.E. Driver, C.C. Mello, Potent and specific genetic interference by double-stranded RNA in *Caenorhabditis elegans*, *Nature* 391 (1998) 806–811.
- [7] K. Gardiner, D. Slavov, L. Bechtel, M. Davison, Annotation of human chromosome 21 for relevance to Down syndrome: gene structure and expression analysis, *Genomics* 79 (2002) 833–843.
- [8] K. Gardiner, D. Slavov, A. Fortna, Chromosome 21 genes; homologues in yeast, *C. elegans*, *Drosophila*, zebrafish, and mouse, *Cytogenet. Cell Genet.* 92 (2000) 11.
- [9] Y. Gitton, N. Dahmane, S. Baik, I.A.A. Ruiz, L. Neidhardt, M. Scholze, B.G. Herrmann, P. Kahlem, A. Benkahla, S. Schrinner, R. Yildirimman, R. Herwig, H. Lehrach, M.L. Yaspo, A gene expression map of human chromosome 21 orthologues in the mouse, *Nature* 420 (2002) 586–590.
- [10] M. Guipponi, K. Brunschwig, Z. Chamoun, H.S. Scott, K. Shibuya, J. Kudoh, A.-L. Delezoide, S. El Samadi, Z. Chettou, C. Rossier, N. Shimizu, F. Mueller, J.-M. Delabar, S.E. Antonarakis, C21orf5, a novel human chromosome 21 gene, has a *Caenorhabditis elegans* ortholog (pad-1) required for embryonic patterning, *Genomics* 68 (2002) 30–40.
- [11] R.S. Haltiwanger, Regulation of signal transduction pathways in development by glycosylation, *Curr. Opin. Struct. Biol.* 12 (2002) 593–598.
- [12] M. Hattori, A. Fujiyama, T.D. Taylor, H. Watanabe, T. Yada, H.S. Park, A. Toyoda, K. Ishii, Y. Totoki, D.K. Choi, Y. Groner, E. Soeda, M. Ohki, T. Takagi, Y. Sakaki, S. Taudien, K. Blechschmidt, A. Polley, U. Menzel, J. Delabar, K. Kumpf, R. Lehmann, D. Patterson, K. Reichwald, A. Rump, M. Schillhabel, A. Schudy, W. Zimmermann, A. Rosenthal, J. Kudoh, K. Schibuya, K. Kawasaki, S. Asakawa, A. Shintani, T. Sasaki, K. Nagamine, S. Mitsuyama, S.E. Antonarakis, S. Minoshima, N. Shimizu, G. Nordsiek, K. Hornischer, P. Brant, M. Scharfe, O. Schon, A. Desario, J. Reichelt, G. Kauer, H. Blocker, J. Ramser, A. Beck, S. Klages, S. Hennig, L. Riesselmann, E. Dagand, T. Haaf, S. Wehrmeyer, K. Borzym, K. Gardiner, D. Nizetic, F. Francis, H. Lehrach, R. Reinhardt, M.L. Yaspo, The DNA sequence of human chromosome 21, *Nature* 405 (2000) 311–319.
- [13] R.S. Kamath, M. Martinez-Campos, P. Zipperlen, A.G. Fraser, J. Ahringer, Effectiveness of specific RNA-mediated interference through ingested double-stranded RNA in *Caenorhabditis elegans*, *Genome Biol.* 2 (2001) (RESEARCH0002).
- [14] R. Kleene, E.G. Berger, The molecular and cell biology of glycosyltransferases, *Biochim. Biophys. Acta* 1154 (1993) 283–325.
- [15] M. Labouesse, S.E. Mango, Patterning the *C. elegans* embryo: moving beyond the cell lineage, *Trends Genet.* 15 (1999) 307–313.
- [16] T. Lubke, T. Marquardt, K. von Figura, C. Korner, A new type of carbohydrate-deficient glycoprotein syndrome due to a decreased import of GDP-fucose into the Golgi, *J. Biol. Chem.* 274 (1999) 25986–25989.
- [17] K. Luhn, M.K. Wild, M. Eckhardt, R. Gerardy-Schahn, D. Vestweber, The gene defective in leukocyte adhesion deficiency II encodes a putative GDP-fucose transporter, *Nat. Genet.* 28 (2001) 69–72.
- [18] M. Maduro, D. Pilgrim, Identification and cloning of unc-119, a gene expressed in the *Caenorhabditis elegans* nervous system, *Genetics* 141 (1995) 977–988.
- [19] S.M. Magdaleno, T. Curran, Gene dosage in mice—BAC to the future, *Nat. Genet.* 22 (1999) 319–320.
- [20] I. Martinez-Duncker, R. Mollicone, J.J. Candelier, C. Breton, R. Oriol, A new superfamily of protein-O-fucosyltransferases, {alpha}2-fucosyltransferases, and {alpha}6-fucosyltransferases: phylogeny and identification of conserved peptide motifs, *Glycobiology* 13 (2003) 1C–5C.
- [21] C.C. Mello, J.M. Kramer, D. Stinchcomb, V. Ambros, Efficient gene transfer in *C. elegans*: extrachromosomal maintenance and integration of transforming sequences, *EMBO J.* 10 (1991) 3959–3970.
- [22] W.A. Mohler, J.S. Simske, E.M. Williams-Masson, J.D. Hardin, J.G. White, Dynamics and ultrastructure of developmental cell fusions in the *Caenorhabditis elegans* hypodermis, *Curr. Biol.* 8 (1998) 1087–1090.
- [23] R.J. Mural, M.D. Adams, E.W. Myers, H.O. Smith, G.L. Miklos, R. Wides, A. Halpern, P.W. Li, G.G. Sutton, J. Nadeau, S.L. Salzberg, R.A. Holt, C.D. Kodira, F. Lu, L. Chen, Z. Deng, C.C. Evangelista, W. Gan, T.J. Heiman, J. Li, Z. Li, G.V. Merkulov, N.V. Milshina, A.K. Naik, R. Qi, B.C. Shue, A. Wang, J. Wang, X. Wang, X. Yan, J. Ye, S. Yoosheph, Q. Zhao, L. Zheng, S.C. Zhu, K. Biddick, R. Bolanos, A.L. Delcher, I.M. Dew, D. Fasulo, M.J. Flanagan, D.H. Huson, S.A. Kravitz, J.R. Miller, C.M. Mobarry, K. Reinert, K.A. Remington, Q. Zhang, X.H. Zheng, D.R. Nusskern, Z. Lai, Y. Lei, W. Zhong, A. Yao, P. Guan, R.R. Ji, Z. Gu, Z.Y. Wang, F. Zhong, C. Xiao, C.C. Chiang, M. Yandell, J.R. Wortman, P.G. Amanatides, S.L. Hladun, E.C. Pratts, J.E. Johnson, K.L. Dodson, K.J. Woodford, C.A. Evans, B. Gropman, D.B. Rusch, E. Venter, M. Wang, T.J. Smith, J.T. Houck, D.E. Tompkins, C. Haynes, D. Jacob, S.H. Chin, D.R. Allen, C.E. Dahlke, R. Sanders, K. Li, X. Liu, A.A. Levitsky, W.H. Majoros, Q. Chen, A.C. Xia, J.R. Lopez, M.T. Donnelly, M.H. Newman, A. Glodek, C.L. Kraft, M. Nodell, F. Ali, H.J. An, D. Baldwin-Pitts, K.Y. Beeson, S. Cai, et al., A comparison of whole-genome shotgun-derived mouse chromosome 16 and the human genome, *Science* 296 (2002) 1661–1671.
- [24] T. Okajima, K.D. Irvine, Regulation of notch signaling by O-linked fucose, *Cell* 111 (2002) 893–904.
- [25] T. Okajima, A. Xu, K.D. Irvine, Modulation of notch-ligand binding by protein O-fucosyltransferase 1 and fringe, *J. Biol. Chem.* 278 (2003) 42340–42345.

- [26] A. Reymond, A.A. Camargo, S. Deutsch, B.J. Stevenson, R.B. Parmigiani, C. Ucla, F. Bettoni, C. Rossier, R. Lyle, M. Guipponi, S. de Souza, C. Iseli, C.V. Jongeneel, P. Bucher, A.J. Simpson, S.E. Antonarakis, Nineteen additional unpredicted transcripts from human chromosome 21, *Genomics* 79 (2002) 824–832.
- [27] A. Reymond, M. Friedli, C.N. Henrichsen, F. Chapot, S. Deutsch, C. Rossier, C. Rossier, R. Lyle, M. Guipponi, S.E. Antonarakis, From PREDs and open reading frames to cDNA isolation: revisiting the human chromosome 21 transcription map, *Genomics* 78 (2001) 46–54.
- [28] A. Reymond, V. Marigo, M.B. Yaylaoglu, A. Leoni, C. Ucla, N. Scamuffa, C. Caccioppoli, E.T. Dermitzakis, R. Lyle, S. Banfi, G. Antonarakis, S.E. Antonarakis, A. Ballabio, Human chromosome 21 gene expression atlas in the mouse, *Nature* 420 (2002) 582–586.
- [29] A. Reymond, G. Meroni, A. Fantozzi, G. Merla, S. Cairo, L. Luzi, D. Riganelli, E. Zanaria, S. Messali, S. Cainarca, A. Guffanti, S. Minucci, P.G. Pelicci, A. Ballabio, The tripartite motif family identifies cell compartments, *EMBO J.* 20 (2001) 2140–2151.
- [30] J.E. Sulston, E. Schierenberg, J.G. White, J.N. Thomson, The embryonic cell lineage of the nematode *Caenorhabditis elegans*, *Dev. Biol.* 100 (1983) 64–119.
- [31] R.H. Waterston, K. Lindblad-Toh, E. Birney, J. Rogers, J.F. Abril, P. Agarwal, R. Agarwala, R. Ainscough, M. Alexandersson, P. An, S.E. Antonarakis, J. Attwood, R. Baertsch, J. Bailey, K. Barlow, S. Beck, E. Berry, B. Birren, T. Bloom, P. Bork, M. Botcherby, N. Bray, M.R. Brent, D.G. Brown, S.D. Brown, C. Bult, J. Burton, J. Butler, R.D. Campbell, P. Carninci, S. Cawley, F. Chiaromonte, A.T. Chinwalla, D.M. Church, M. Clamp, C. Clee, F.S. Collins, L.L. Cook, R.R. Copley, A. Coulson, O. Couronne, J. Cuff, V. Curwen, T. Cutts, M. Daly, R. David, J. Davies, K.D. Delehaunty, J. Deri, E.T. Dermitzakis, C. Dewey, N.J. Dickens, M. Diekhans, S. Dodge, I. Dubchak, D.M. Dunn, S.R. Eddy, L. Elnitski, R.D. Emes, P. Esvara, E. Eyra, A. Felsenfeld, G.A. Fewell, P. Flicek, K. Foley, W.N. Frankel, L.A. Fulton, R.S. Fulton, T.S. Furey, D. Gage, R.A. Gibbs, G. Glusman, S. Gnerre, N. Goldman, L. Goodstadt, D. Grafham, T.A. Graves, E.D. Green, S. Gregory, R. Guigo, M. Guyer, R.C. Hardison, D. Haussler, Y. Hayashizaki, L.W. Hillier, A. Hinrichs, W. Hlavina, T. Holzer, F. Hsu, A. Hua, T. Hubbard, A. Hunt, I. Jackson, D.B. Jaffe, L.S. Johnson, M. Jones, T.A. Jones, A. Joy, M. Kamal, E.K. Karlsson, et al., Initial sequencing and comparative analysis of the mouse genome, *Nature* 420 (2002) 520–562.
- [32] X.W. Yang, C. Wynder, M.L. Doughty, N. Heintz, BAC-mediated gene-dosage analysis reveals a role for *Zipro1* (*Ru49/Zfp38*) in progenitor cell proliferation in cerebellum and skin, *Nat. Genet.* 22 (1999) 327–335.